Journal of Applied Polymer Science

Design and *in vitro* investigation of nanocomposite hydrogel based *in situ* spray dressing for chronic wounds and synthesis of silver nanoparticles using green chemistry

Arun Kumar, Maneesh Jaiswal
Department of Pharmacy, Jaypee University of Information Technology (JUIT), Waknaghat, Solan, Himachal Pradesh 173234, India
Correspondence to: M. Jaiswal (E-mail: jaiswal.maneesh@gmail.com)

ABSTRACT: An innovative concept of spontaneous film dressing has been designed as sprayed hydrogel dressings (SHD) using a blend of polyvinyl alcohol (PVA) and sodium alginate (SA) as synthetic and natural polymeric components and, were crosslinked with boric acid and calcium chloride, respectively. Silver nanoparticles (AgNPs) are synthesized by green chemistry using *Ficus benghalensis* extract (FB) and were characterized by SEM and zeta sizer. FTIR spectra show polymeric interaction with $AgNP_s$, while SEM images show outer surface of the SHD film. Equilibrium swelling and degradation in aqueous media (distilled water and buffers) are found to be dependent upon PVA/SA ratio. Polymeric combination exhibit pseudoplastic behavior with Farrow's constant >1. Uniformly distributed AgNPs (particle size ~27.55 ± 2.01 nm), high water retention (~13 fold), and biodegradable (~5 days) nature of dressing along with sustained release profile of both AgNPs and extract with concentration-dependent antimicrobial activity have been observed for 24 h. Self shaped, biodegradable, aseptic, prolong anti-oxidative, non-hemolytic, blood compatible, and hemostatic properties of SHD film appears as promising dressing for superficial wounds. © 2015 Wiley Periodicals, Inc. J. Appl. Polym. Sci. **2016**, *133*, 43260.

KEYWORDS: biomaterials; drug delivery systems; gels; hydrophilic polymers; swelling

Received 25 July 2015; accepted 23 November 2015
DOI: 10.1002/app.43260

INTRODUCTION

To meet demand for emerging innovative products, higher cosmetic expectations of patients as well as rising incidence of chronic wounds such as diabetic wounds, pressure ulcers and surgical injury, researchers have to explore novel concepts of skin wounds management.[1] The selection of biomaterials, texture of dressing, and its biochemical properties need to be controlled very precisely as chronic wound healing is a very complex biological process, involves cascade of overlapping events.[2] The complexities of chronic wounds can be resolved through designing of modern dressing which imbibe all the requisite properties and provide an ideal healing environment along with excellent patient convenience.

Moist and aseptic wound microenvironment as well as uninterrupted availability of anti-inflammatory and healing promoting agents in a sustained manner has shown utmost importance for chronic wounds management.[3] Hydrogels are proven formulations in this context with immense water retention properties and tissue mimetic consistency. Commercially, these are available in various branded products in forms of sheets, foam, or gels such as Tegaderm® CHG (3M Healthcare), Vigilon Gel, Lyofoam (Seton Health care), Normlgel (Molnlycke), Ameda Comfort Gel and SPAND-Gel™. Various synthetic polymers such as PVA, poly (caprolactone), polyurethanes, and their combinations with natural counterpart, i.e., gelatin, collagen, chitosan, alginates, and cellulose derivatives have been investigated by various research groups for the development of hydrogel-based dressings. Majority of formulations offered patient inconvenience due to their high thickness, sticking to the wound surface or due to instability under high stresses. In addition, application of secondary dressings causes further trauma at the site.[4] To overcome such complications, researchers have been investigated polymeric biomaterials toward designing of novel dressing with high mechanical property such as nanocomposite hydrogels loaded withclays,[5] crosslinked nonswellable hydrogel with high mechanical property.[6,7] Sun *et al.* synthesized a new class of viscoelastic hydrogels from polyampholyteswith tunable mechanical properties.[8] Gong *et al.* synthesized double network hydrogels as a substitute for articular cartilage and connective tissue using combination of hydrophilic polymers with extremely high mechanical property, swelling (60–90%) and also showed high wear resistance due to their extremely low coefficients of friction.[9] Balakrishnan *et al.* developed *in situ* forming hydrogel dressing using gelatin, oxidized alginate, and borax which have showed enhanced migration of epithelial cell

in full thickness rat model.[10] Bioactive injectable hydrogel dressing was developed by Dong *et al.* using polyethylene glycol (PEG)-based thermo responsive hyper-branched copolymer and thiol-modified hyaluronic acid for wound healing applications.[11] Long-term viability of adipose derived stem cells and prevention of unwanted wound contraction was achieved which may otherwise cause scars, painful contractures and mobility dysfunction in the cases of large, deep wounds such as extensive burns.

Silver nanoparticles are broad spectrum antimicrobial agents against resistant species and are economically available as various brand names such as Allevyn Ag, Actisorb Silver (Smith & nephew), Polymem (Ferris Mfg. Corp.), Contreet (Coloplast) and many more brands. The synthesis technique and local toxicity of silver are major concern for its biological application as reduction of silver salt using synthetic chemicals such as sodium borohydride is hazardous to environment, while high concentration of silver in wound tissue adversely affects nascent tissues and thus hamper the healing progression.[12]

To overcome these issues, present research work utilized green chemistry of *FB* extract (a natural reducing agent) for synthesis of AgNPs, while instability problems and concentration-dependent toxicity issue was controlled by sustaining its release using a crosslinked network of PVA and SA. Furthermore, *in situ* sprayed hydrogel film was developed in association with AgNPs to provide mechanical strength to the film. The *FB* extract was utilized as an antioxidant as well as hemostatic agent which immediately coagulate the blood and acts against oxidative stress on its application in a cost effective and sustained manner. PVA is a biocompatible and chemically neutral polymer which has widely explored for drug delivery and biomedical applications. It is an excellent film forming agent and able to maintain a continuous moist environment around the wound surface while, SA is a natural polysaccharide possessing high gel forming ability, biocompatible, high protein adsorption ability.[13]

In this research work, extensive *in vitro* investigations have been carried out for physico-chemical and biological properties of PVA/SA sprayed films such as swelling behavior, degradation study, polymeric interaction through TGA and FTIR, surface morphology by SEM, silver content by atomic adsorption spectroscopy, release profile of AgNPs and *FB* extract followed by protein absorption, hemocompatibility, *in vitro* antimicrobial and hemostatic activity of extract loaded sprayed films through various sophisticated tools.

EXPERIMENTAL

Materials

PVA (mol. weight ~77,000 g mol^{-1}), sodium dodecyl sulfate and sodium alginate (SA) were purchased from (Loba Chemie, Mumbai, India), calcium chloride (Merck specialties, India), 2,2-diphenyl-1-picrylhydrzyl and bovine serum albumin (Himedia, Mumbai), methanol, nitric acid, hydrochloric acid, and boric acid were purchased from (Merck, Mumbai, India), silver nitrate, ethylenediamine tetra acetic acid (EDTA), sodium chloride (Fisher Scientific, Mumbai, India) and all other chemicals and reagents were of analytical grade. Double distilled water was used throughout the investigation and preparation of solutions.

Methods

Synthesis of Silver Nanoparticles. For the preparation of silver nanoparticles, green synthesis method was used. Briefly, varying concentration (i.e., 2–% w/v) of aqueous solution of *FB* extract was added with equal volume of 1 m*M* aqueous silver nitrate solution (5 mL) and allowed to react at 45°C under continuous stirring. Periodic sampling was carried out after 0, 10, 20, and 25 min in order to monitor the change in color and UV absorbance of the solution.[14]

Characterization of Silver Nanoparticles (AgNPs). ***Particle size, zeta potential, and UV spectroscopy analysis.*** Droplet size and zeta potential of AgNPs were observed using Nanotrac Wave Zetasizer (Microtrac, USA) at room temperature at an angle of 180°.

In Vitro* Antimicrobial Activity.** ***Test microorganisms and growth media. *E. coli* (ATCC-723) and *S. aureus* (MTCC-3160) were chosen based on their pharmacological and clinical importance. Nutrient broth was used as a growth medium for growing these cultures at 37°C for 24 h and stored at 4°C until further use. The growth in the culture medium was assessed based on turbidity appearance.

Minimum Inhibitory Concentration (MIC) of Silver Nanoparticles. This method was based on the broth dilution assay.[15] Serial dilutions were made by mixing PBS (900 μL) from the stock solution and bacterial culture grown in nutrient broth (100 μL). From this solution, 100 μL of the mixture was again mixed with 900 μL of PBS (10^{-1}) and which was further diluted to get a maximum diluted concentration of 10^{-9}. The control plates (without AgNPs) were prepared by spreading 100 μL of culture (micro-organism) made in PBS (i.e., 10^{-2}, 10^{-4}, 10^{-5}, 10^{-6}, and 10^{-8}) to get countable colonies (150–200). The test agar plates were prepared by mixing and pouring different concentration of AgNPs (test) with that of nutrient agar followed by spreading of culture (10^{-5}). The concentration of AgNPs at which no colony remains on the culture plate, was chosen as MIC of AgNPs and that amount was loaded in the PVA/SA sprayed hydrogel dressing (SHD).

Preparation of PVA/SA Sprayed Hydrogel Films. Physically crosslinked gels of PVA and sodium alginate (SA) solution were prepared using boric acid and $CaCl_2$, respectively in specific ratios. Briefly, aqueous solution of PVA (6% w/v), sodium alginate (3% w/v), $CaCl_2$ (3% w/v), and boric acid (8% w/v) solution was prepared by dissolving them in distilled water. Varying ratio of PVA/SA (1:1, 1:2, 1:3, 2:1, 3:1, and 4:1) containing specific amount of AgNPs and *FB* extract were mixed thoroughly and sprayed films were prepared by spraying the mixture of both the polymers (PVA & Sodium Alginate) and cross-linkers ($CaCl_2$& boric acid) simultaneously on a glass slide. Films were peeled out and kept in freeze till further studies.

Physicochemical Characterization of Spray Hydrogel Dressing (SHD). ***Fourier-transform infrared spectroscopy (FTIR).*** All samples were dried by lyophilization (Alpha 1-2 LD plus, Germany) and crushed to get fine powder for further analysis. The

FTIR spectrums were obtained by recording bands between 4000 and 400 cm^{-1} with a resolution of 2 cm^{-1}.

Scanning electron microscopy (SEM). The surface and internal morphology of the SHD films were investigated by analytical SEM with 15 kV voltages for secondary electron imaging. The sprayed films were made by snap freezing method using liquid nitrogen and coated with gold using an ion sputter coater (Hitachi S3400N, US) lyophilized before lyophilization.

Thermal gravimetric analysis (TGA). TGA analysis of the blank and AgNPs loaded SHD film was performed using a TGA-Pyres-6TGA (EXSTAR TG/DTA 6300, Woodland, CA) by heating the sprayed films from 50 to 750°C at a heating rate of 20°C min^{-1} under a nitrogen flow. A derivative plot was used to calculate the initial (T_i), maximum (T_{max}) and final decomposition (T_f) temperatures of the sprayed films.

Determination of swelling behavior. For determination of swelling behavior, the SHD films were kept in petri plates and dried at 40°C for 4 h. Briefly, dried samples (W_e; ~10 mg) of SHD films were immersed in distilled water and buffers (pH 1.2, 6.5, and 7.4). At predetermined time intervals of 1, 3, 6, 12, and 24 h, swollen disks were weighed (W_s) on analytical balance ($n = 3$, after blotting on filter paper), till constant weight is achieved. Water uptake capacities of SDH specimens were determined using following equation.[16]

$$\text{Equilibrium swelling ratio (\% ESR)} = \frac{W_s - W_e}{W_e} \times 100$$

In vitro weight loss profile. The *in vitro* weight loss profile of SHD films was studied by measuring the change in weight as a function of time.[17] SHD specimens were placed in petri plates containing distilled water and phosphate buffer (pH 6.5) separately, and incubated at 37°C ± 0.2°C at 50 rpm in an incubator shaker (Labnet 311DS, USA). At a predetermined time interval, fresh medium was added (replaced) and films were weighed and the percentage weight loss was calculated using the following formula:

$$\%\ \text{Degradation} = \frac{\text{Wt}_{(i)} - \text{Wt}_{(t)}}{\text{Wt}_{(t)}} \times 100$$

Where $\text{Wt}_{(t)}$ is the weight of the films at time t and $\text{Wt}_{(i)}$ is the initial weight of the films at time zero.

Effect of PVA concentration on to the rheological property of SHD films. The flow property of the PVA and AgNPs solution (2, 4, and 8% w/v) was studied using Brookfield viscometer (RVT, Brookfield Engineering Laboratories, USA) at a rotation speed of 20 rpm using spindle no 64. The corresponding dial reading was noted to get viscosity value. The viscosity values obtained was used to calculate the Farrow's constant (indicator of pseudo-plasticity).

Atomic absorption spectroscopy, drug loading and in vitro release studies. Atomic absorption spectroscopy were performed to find out the distribution pattern and content uniformity of AgNPs within SHD using three randomly selected sites of the film. Specimens were prepared by boiling the dried weighted SHD discs in aqua regia (mixture of nitric acid and hydrochloric acid; 1:3). A flame atomic absorption spectrophotometer (AAS) (Perkin Elmer 3100, MA) was used with a silver hollow cathode-lamp, at an operating current of 2 mA, a wavelength, and a spectral bandwidth of 328.1 and 0.2 nm, respectively. For standard specimens, AgNPs prepared by chemical reduction method using sodium borohydride (0.1 mg mL^{-1}) were used.

To determine the distribution and content of *FB* extract in sprayed film, dried specimens were incubate in 50 mL buffer (pH 7.4) to swell followed by centrifugation for 15 min at 13,000 rpm in order to leach out the extract from the hydrogels. The solution was filtered and analyzed using UV spectrophotometer (λ_{max}, 275 nm). The percentage loading was calculated using the equation.[18]

$$\%\ \text{Drug loading} = \frac{\text{Wt}_{(\text{drug in film})}}{\text{Wt}_{(\text{film})}} \times 100$$

The *in vitro* release profile of *FB* extract and AgNPs from the films was carried out using dialysis membrane (cellulose nitrate membrane; pore size 0.22 μm) and Franz diffusion cell.[19] The cell consists of two chambers, (1) the donor compartment was open from the top and exposed to atmosphere while, (2) the receptor compartment consists of sampling port and release medium (pH 6.5; 37°C ± 0.5°C). The SHD specimens were placed on the donor compartment and, at a predetermined time interval, i.e., 0.5, 1, 2, 4, 6, 8, 10, 12, 14, and 24 h, 1 mL samples were withdrawn and replaced by the same amount of the fresh medium to maintain sink condition. Samples were analyzed for content release (i.e., FB extract and AgNPs) under UV spectrophotometer at λ_{max}, 275 and 430 nm, respectively.

Biological Evaluation of Hydrogel Film. ***Hemocompatibility study.*** The blood compatibility of SHD films (loaded with AgNPs and FB extract) was carried out using elution method reported by Chhatri *et al.* and Singh *et al.*[20,21] Accordingly, film specimens were first equilibrated with normal saline (0.9% NaCl at 37°C) for 24 h followed by incubation in PBS (pH 7.4) for 72 h. The elute was removed after centrifugation at 3000 rpm for 20 min and 1 mL of blood (containing anti-coagulant) was added. It was kept at 37°C for 3 h followed by centrifugation at 3000 rpm for 20 min. Nearly 1 mL of Triton X and PBS (pH 7.4) were used as positive and negative controls, respectively. The supernatant containing hemoglobin released by hemolysis was calculated by measuring the absorbance at 540 nm. The percentage hemolysis was calculated by using the equation:

$$\text{Hemolysis (\%)} = \frac{A_{(\text{Sample of film})} - A_{(\text{negetive control})}}{A_{(\text{Positive control})} - A_{(\text{negetive control})}} \times 100$$

where $A_{(\text{sample of film})}$ is the absorbance of tested material sample while $A_{(-)\ \text{control}}$ and $A_{(+)\ \text{control}}$ are the absorbance of –ve and +ve control. According to their hemolytic activity, the results of hemolysis test were classified into three types as follows: (a) hemolytic materials have hemolysis >5%, (b) slightly hemolytic material having hemolysis between 2 and 5%, and (c) nonhemolytic materials have hemolysis <2%.[22]

In vitro hemostatic activity: Coagulation time determination. Blood samples were collected from local slaughter house (Solan, HP, India) in blood bottles containing ethylene diamine tetra acetic acid (EDTA) as an anticoagulant. Coagulation time was determined according to the protocol mentioned by Behrens

et al.[23] Briefly, 0.5, 1, and 2 mL of anti-coagulated blood was added into three different vials containing FB extract (20 mg), sprayed films (blank), and film loaded *FB* extract (~100 mg of dry weight equivalent to 20 mg extract). Samples in the vials were recalcified with 10 m*M* $CaCl_2$ solution. The vials were inverted after every minute in order to check the clotting of the blood and the time were recorded. All experimental and control groups were run in triplicate ($n = 3$).

Study of protein absorption on to the surface of SHD. The amount of protein adsorbed was determined using UV spectrophotometer according to the method reported by Lin *etal.*[24] SHD film specimens were cut into square shape (1×1 cm^2) and immersed in 5 mL of phosphate buffer saline (PBS) pH 7.4 containing 30 mg mL^{-1} of bovine serum albumin (BSA) under shaking (50 rpm) for 4 h at 37°C. Afterward, samples were taken out gently and rinsed three times with PBS to detach loosely attached protein followed by extraction of surface protein by 1% (w/v) aqueous solution of sodium dodecyl sulfate (SDS) under stirring for 1 h at room temperature. The adsorbed protein content onto the film was calculated by plotting calibration curve of BSA in SDS solution using UV absorbance at λ_{max} 630 nm.[24]

In vitro free radical scavenging activity. Sustained release of FB extract and prolong oxidation stress free environment in the wound milieu were desirable for long term utility of the dressing. The free radical scavenging activity of released extract from the SHD was calculated with respect to time using DPPH (2,2-diphenyl-1-picrylhydrazyl) scavenging assay as reported by Mahdi *et al.*[25] A 500-µL sample of *FB* extract specimens (collected from the release medium) was added to 1 mL of 0.1 m*M* w/v alcoholic solution of DPPH. The solution was incubated for 30 min in dark at room temperature and then measured UV absorbance at 517 nm λ_{max}. The results were expressed as "percentage of DPPH reduced" using the following equation where A_0 was the absorbance of the control i.e., DPPH alone and, A_1 was the absorbance of the test i.e., *FB* extracts released from the hydrogel films. Each experiment was conducted in triplicate ($n = 3$) and results were shown as ± standard deviation.[25]

$$\text{Percentage inhibition} = \frac{\text{A0-A1}}{\text{A0}} \times 100$$

In Vitro* Antimicrobial Activity. *Microbial penetration. The microbe penetration test was performed as reported by Kokabi *et al.* to evaluate the physical resistance of formulated PVA/SA hydrogel films against microbe's transmission from the environment to the wound surface.[26] Circular pieces of SHD film (diameter ~5 cm and thickness ~3 mm) were washed with deionized water and sterilized under UV light for 1 h. The sterilized samples were placed on the nutrient agar followed by a drop (concentration of 10^9 mL^{-1}) of bacterial suspension (*S. aureus*) on the top of the film and incubated it at 37°C (temperature for the growth of bacteria) in an incubator. The film samples were visually monitored for a week on a regular basis for the presence of bacterial growth on nutrient agar medium beneath the film.

Determination of zone of inhibition. The zone of inhibition (ZOI) due to the presence of antimicrobial AgNPs was determined using agar-well diffusion assay.[27] Nearly 20 µL of microbial culture was inoculated in presterilized glass petri plates containing solidified media. A 6-mm holes were developed using metallic punches and filled them with (i) *FB* extract (E) solution in dimethyl sulfoxide (DMSO) (1 mg mL^{-1}), (ii) AgNPs (10.8 μg mL^{-1}), and (iii) DMSO; negative control; C) while (iv) SHD discs containing AgNPs were placed on the inoculated agar plates without creating holes. All test specimens were kept for incubation for 24 h at 37°C and zone of inhibition was observed. The antimicrobial efficiency of the specimens was measured as the diameter of the zone of inhibition in comparison to negative control. The same procedure was followed for the determination of zone of inhibition of Ag ions released from the SHD samples.

RESULTS AND DISCUSSION

Sprayed hydrogel dressing has been a novel approach in wound management as it will offer a tunable, contamination free, self-shaped protective covering without wrinkling or fluting in the wound bed with excellent patient compliance. In addition, it was biocompatible and biodegradable in nature, as well as was designed to maintain moist, anti-oxidative and continuous sterile environment in the wound milieu.

Synthesis of Silver Nanoparticles, Particle Size, and *In Vitro* Antimicrobial Activity

AgNPs was fabricated by reduction of aqueous solution of silver nitrate (1 m*M*) by varying quantity of *FB* extracts (natural reducing agent) (2, 4, and 6 mg mL^{-1}). AgNPs exhibited brownish color and showed intense absorption spectra in the range of 410–430 nm due to surface Plasmonexcitation vibrations in the metal nanoparticles as shown in Figure 1 (A). The particle size was found in the range of 27.55 ± 2.01 nm [Figure 1(D)] with pdi of 0.66. FB extract acted as a natural reducing agent owing to the presence of tannins, polyphenols such as flavonoids, saponins, and anthocyanin derivatives.[28] These phytochemicals not only convert $AgNO_3$ into AgNPs but also are expected to reduce the *in vivo* oxidative stress, crucial for wound healing progress. Among these, various natural and synthetic hydrophilic polymers containing hydroxyl (—OH), carboxylic (—COOH), amino ($—NH_2$), or thiol groups offers reduction capabilities and in addition stabilize the AgNPs.[29] Based on the above information it was considered that presence of hydroxyl groups along with carbohydrates in FB extract, is capable of effective reduction as well as stabilization of AgNPs.

The countable colony of bacteria was attained by sequential dilution. Culture of 10^{-5} dilution was used for assessment of MIC of the nanoparticles, as countable colonies (i.e., 143) were observed at that dilution. MIC of AgNPs against *S. aureus* and *E. coli* was observed as 47 and 61 µg mL^{-1} of AgNPs [Figure 2(A–D)]. Silver ions (Ag^+) is antimicrobial in nature while it is unstable to store as such, therefore, Ag NPs (Ag^+) have been stored as reservoir of Ag^+ which on release in the medium, acted as antimicrobial agent. AgNPs showed this activity in size as well as concentration-dependent manner.[30] The variation in the MIC of gram positive and gram negative bacteria to silver

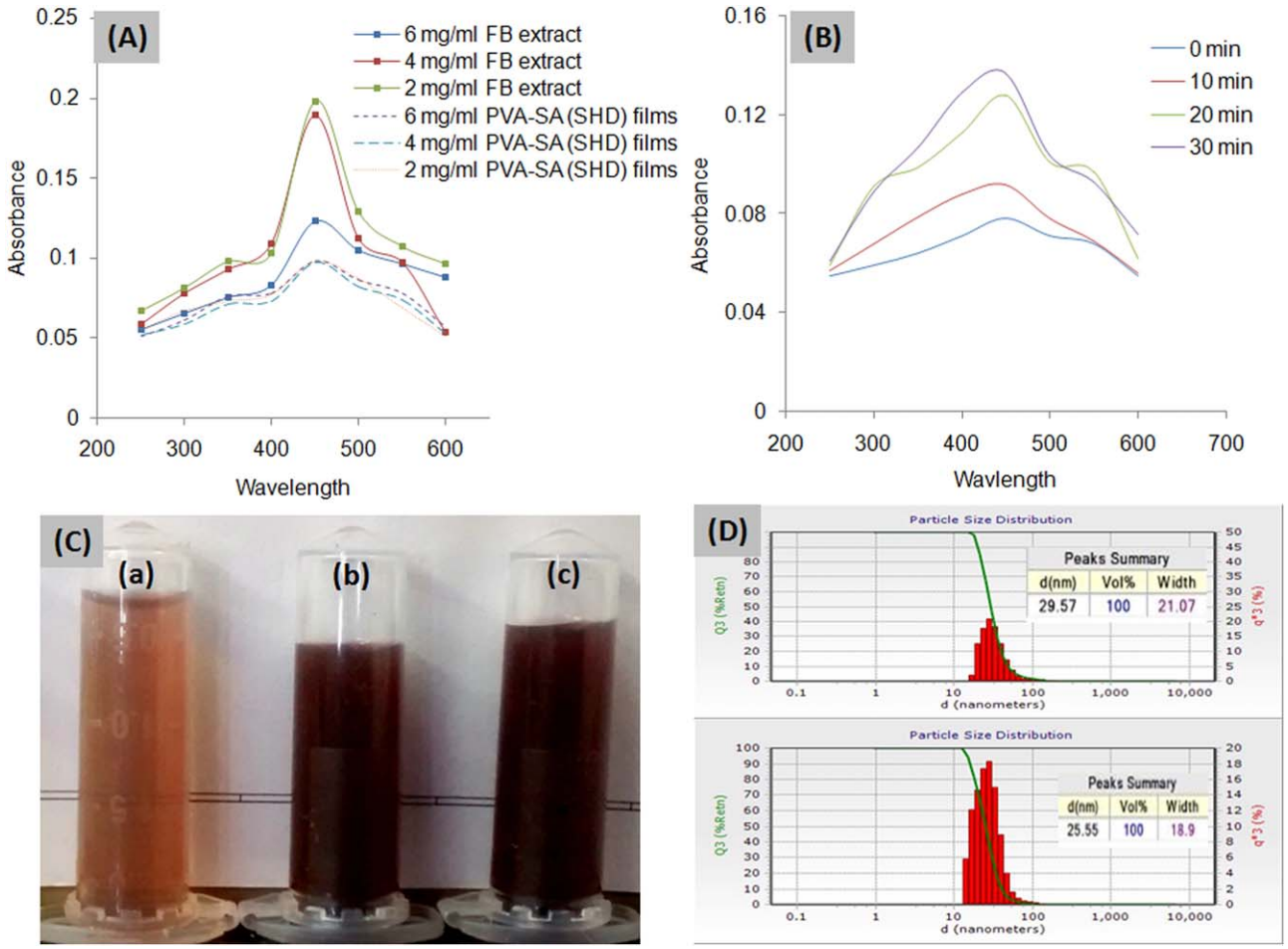

Figure 1. Green synthesis of AgNPs using *FB* extract demonstrated (A) UV–visible spectra of AgNPs from its solution and from PVA/SA SHD films, (B) UV–Visible spectra of AgNPs after 0, 5, 10, and 20 min during synthesis, (C) Photographic images of FB extract (a), AgNPs synthesized using 4 and 6 mg mL^{-1} of *FB* extract [(b) and (c) respectively] and, (D) bar graph showed particle size of AgNPs. [Color figure can be viewed in the online issue, which is available at wileyonlinelibrary.com.]

nanoparticles was due to the difference in the thickness, susceptibility, and constituents of their membrane structure.

Synthesis of PVA/SA Sprayed Hydrogel (SHD) Film

In situ sprayed hydrogels films of PVA/SA loaded with AgNPs were synthesized using a blend of boric acid and calcium chloride as crosslinker, respectively. During film formation, two moles of PVA containing hydroxyl groups were crosslinked with acidic groups of boric acid, while SA containing carboxylic groups (—COOH) were crosslinked with Ca^{+2} ions of calcium chloride thus formed crosslinked polymeric network (IPN)[31,32] (Figure 3).

However, the rate of crosslinking was not significantly affected by the concentration of AgNPs used, but films containing AgNPs retained their shape better, in terms of their flexibility and elasticity than films without AgNPs. Maximum crosslinking (i.e., stable film) required ≥8% BA and ~3% $CaCl_2$ concentration that took ~5–10 s to develop as a film. Figure 4(A) showed spray systems used to spray the mixture of (i) SA/PVA, (ii) BA/$CaCl_2$ (B), and (C) prepared sprayed hydrogel films; while the inset image showed the flexibility and elasticity of prepared films, respectively. Boric acid and calcium chloride being water soluble crosslinkers and offered an advantage of initiating crosslinking of PVA and SA within few seconds, at room temperature. With consideration of needful biocompatibility, mechanical strength as well as swelling and degradation profile, SA was selected for the synthesis of SHD as one of the natural, biocompatible, hydrophilic, and relatively economic polymer and has been investigated for wound dressing application along with PVA due to its high swelling, flexible nature which impacts the limited wound environment away from moisture management.[33]

Physicochemical Characterization of SHD Films

Fourier Transform Infrared Spectroscopy (FTIR). Figure 5(a–d) depicted ATR-FTIR spectra of PVA/SA film (without AgNPs), PVA, SA, and PVA/SA/AgNPs containing film, respectively. The FTIR spectra of PVA [Figure 5 (b)] showed characteristics broad spectrum band at 3300 cm^{-1} (—OH stretching), 2918 cm^{-1} (symmetric —CH_2—) and at 1418 and 1093 cm^{-1} for C—O groups. Sodium alginate [Figure 5(c)] showed its characteristics band at 2931 cm^{-1} and is assigned for —CH_2 group, while 1614, 1416, and 1306 cm^{-1} was due to the presence of carboxyl

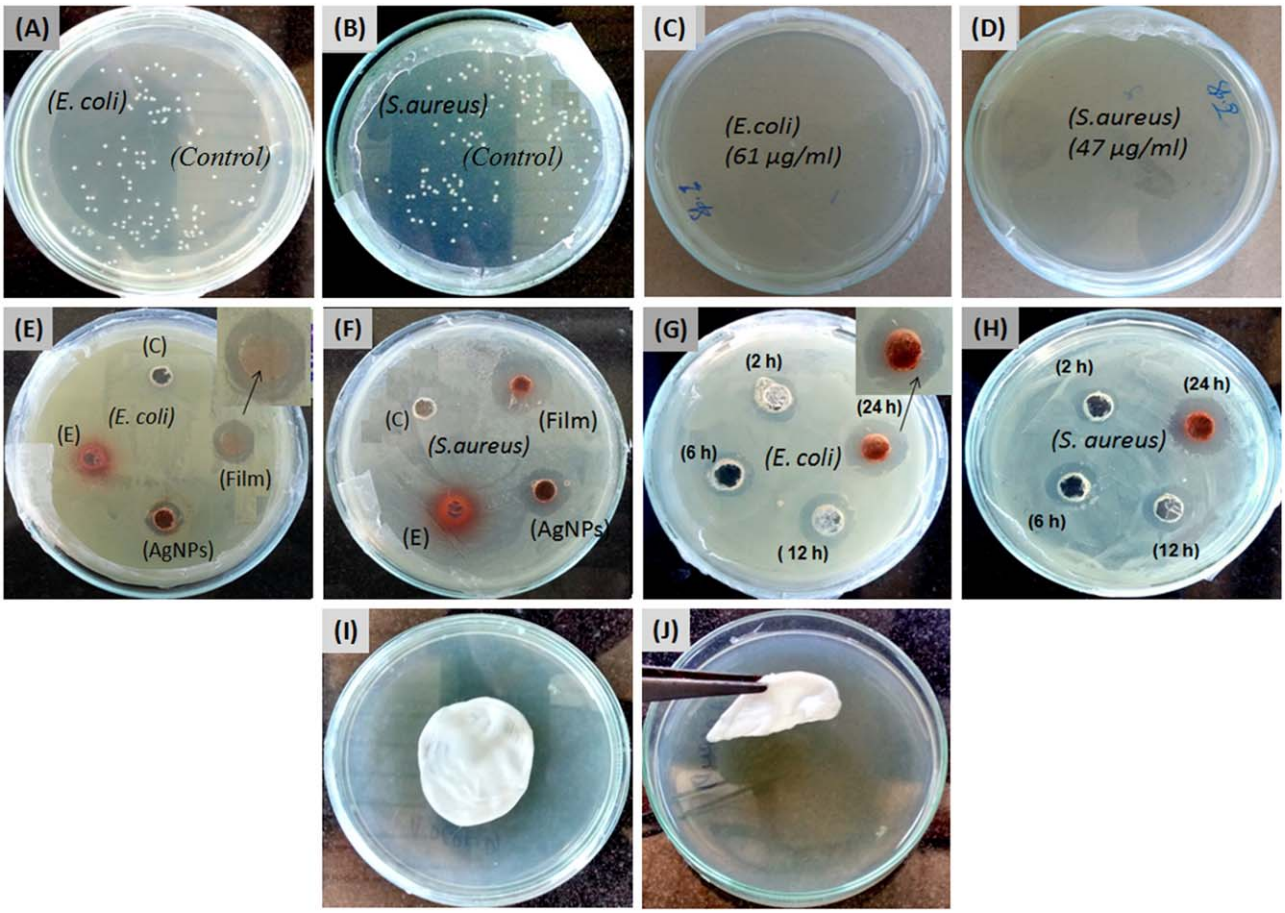

Figure 2. Photographs A–D shows MIC of AgNPs against *E. coli* and *S. aureus* in comparison to blank, figure (E and F) shows zone of inhibition (ZOI) of FB extract, AgNPs, and PVA/SA/Ag SHD films against *E. coli* and *S. aureus,* (G&H) showed the ZOI by Ag ions released from sprayed hydrogel after 2, 6, 12, and 24 h, respectively, while (I and J) showed impermeability of bacteria across the SHD films after 1 week. [Color figure can be viewed in the online issue, which is available at wileyonlinelibrary.com.]

anions (asymmetric and symmetric stretching vibrations). Figure 5(a) showed FTIR spectra of PVA/SA film (without AgNPs). Characteristic bands of —OH and (—CH_2—) were also observed in the spectrum with higher intensity. In this spectrum, characteristic bands of —OH and —COOH (of PVA and sodium alginate) was observed at 1614, 1418, 1306, and 1093 cm^{-1} (indicated by black arrow).[34] Figure 5(d) depicted FTIR spectra of PVA/SA film with AgNPs. The characteristic features of SA and SHD were similar to blank film except lower intensity stretching band of —OH (indicated by green arrow), indicated the probable interaction between the reduced silver ions and —OH of the PVA, and carboxylate group of sodium alginate. It has been found from the figure that the —COO— band of silver film has been shifted to higher wave number i.e., from 1614 to 1670 cm^{-1} (indicated by blue arrow) indicated a strong interaction between SA, PVA, and AgNPs. This shifting can be attributed to the formation of coordination bond between the electron rich groups (such as —C═O and —OH) present in the SHD hydrogel network.

Scanning Electron Microscopy (SEM). Figures 6(A–F) depicts the surface morphology of PVA/SA SHD films with varying PVA/SA ratio i.e., 1:0, 0:1, 1:2, 1:1, 2:1, and 3:1, respectively. The prepared films showed a wrinkled, porous surface with uniformity which may have participated in sustained release of the FB extract and Ag nanoparticles. In matrices A, D, E, and F, small pores as well as crosslinked network were observed (marked by orange arrows). It was found that crosslinked network and pore size were increased with increasing PVA content (PVA/SA) of the films which could be due to the higher hydrophilicity of PVA and crosslinking effect of BA, respectively. On the other side, the uniformity and crosslinked network of the prepared SHD films indicated the physical interaction (i.e., hydrogen bonds) among the functional groups of the blended component.[35] Higher the swelling with increasing PVA content also resulted in the formation of larger ice crystal during snap freezing process. The less porous structure of PVA/SA film with high SA content (0:1 and 1:2) could be due to the formation of amorphous like structure and big difference in the miscibility degree between PVA and SA which further produces different surface porosity, roughness and shrinking of SHD membranes at higher cross-linking density.[36]

Thermo Gravimetric Analysis (TGA). To investigate the polymeric interactions and the effect of Ag on polymeric thermal stability, TGA analysis (i.e., change in physical and chemical

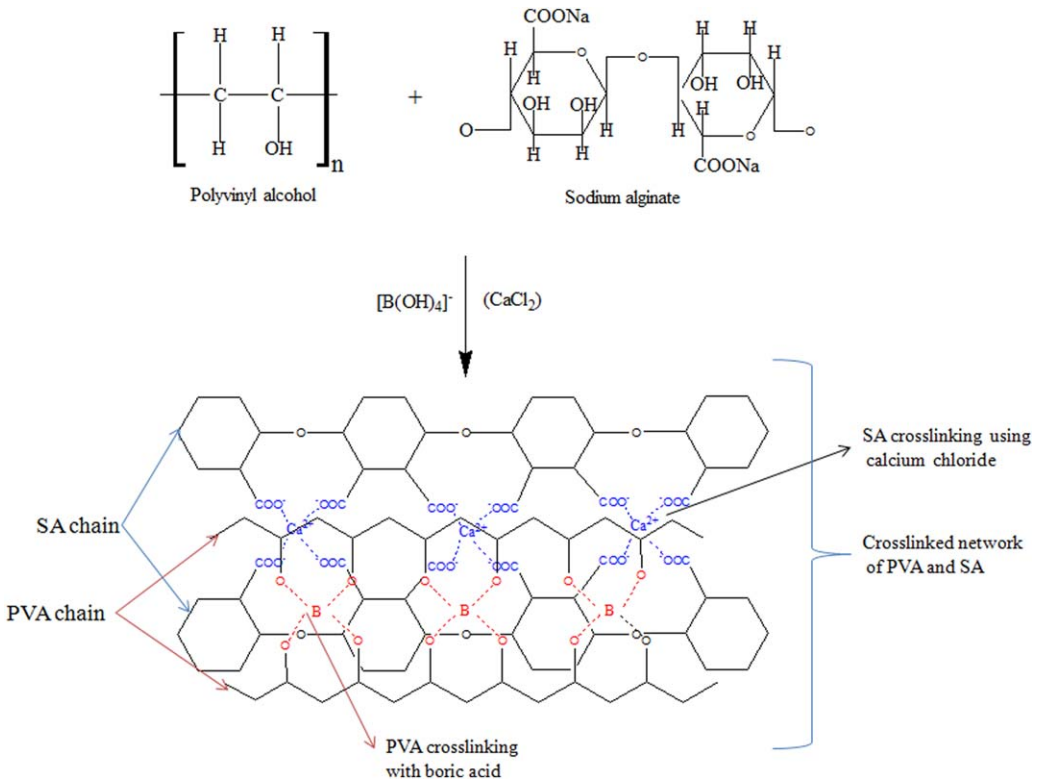

Figure 3. Schematic representation of synthesis of crosslinked SHD film of PVA/SA through crosslinking with $CaCl_2$ and boric acid, respectively. [Color figure can be viewed in the online issue, which is available at wileyonlinelibrary.com.]

property of the materials are recorded as a function of temperature) were performed with PVA, SA alone, blank SHD films and SHD film loaded with AgNPs at a heating rate of 10°C min^{-1} [Figure 7(A–D)]. The TG curve of PVA and SA alone [Figure 7(A,B)] indicated the first decomposition at a range of 30–250°C and 27–100°C was accompanied by 5.34 and 9.47% weight loss. This stage corresponds to loss of physical water present in the PVA and SA. The second decomposition of PVA and SA alone started at 250 and 200°C and ending at 700°C, corresponds to around ~97% and ~72% of weight loss and was indicated by vaporization and burning of volatile part produced by the thermal decomposition of the polymeric chain.[37] The second decomposition was primarily due to the chain scission, subsequent side reactions like cyclization, crosslinking, and partial carbonization.[38]

DTG (differential thermal gravimetery) curve was used to identify the temperature at which maximum weight loss was observed as an indication of polymeric interaction. The T_{DTG} (i.e., the temperature at which maximum weight loss was observed by PVA and SA alone) was found to be 293°C (1.45 mg min^{-1}) and 247°C (0.64 mg min^{-1}) respectively, which may correspond to loss of lattice water. Differential thermal analysis

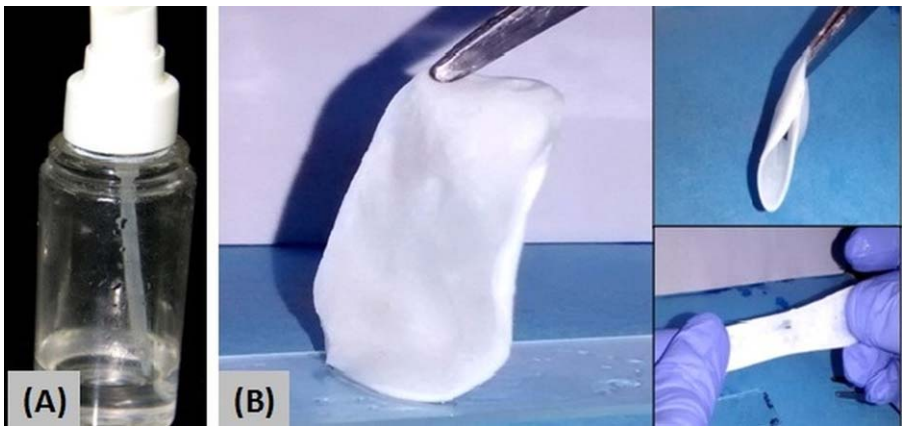

Figure 4. Photograph of SHD films demonstrated (A) sprayer used for spraying mixture of polymers and crosslinkers, (B) strength of SHD film (image showed flexibility and elasticity of SHD films). [Color figure can be viewed in the online issue, which is available at wileyonlinelibrary.com.]

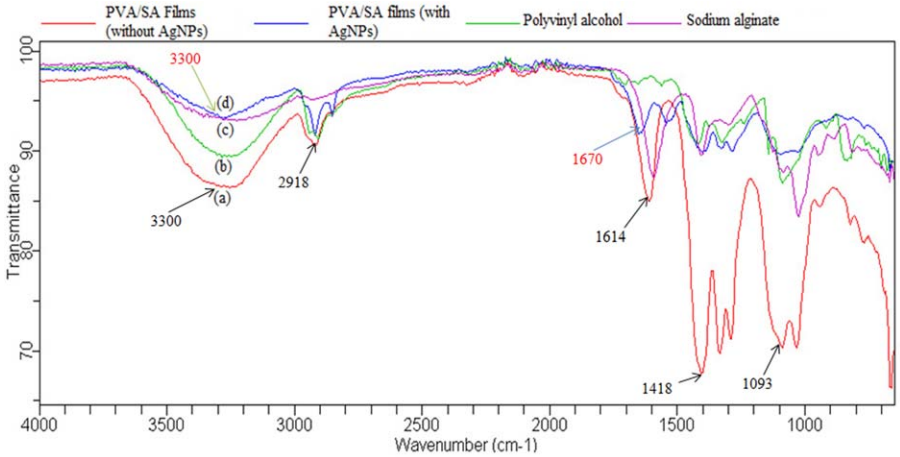

Figure 5. Demonstration of comparative ATR-FTIR spectra of (a) PVA/SA SHD films (without AgNPs), (b) PVA, (c) Sodium alginate (SA) and (d) PVA/SA film with AgNPs. [Color figure can be viewed in the online issue, which is available at wileyonlinelibrary.com.]

(DTA) is used to record the temperature difference between the samples and reference followed by detection of the exothermic and endothermic weight loss. Two peaks were observed for PVA alone i.e., at 223°C (5.99 uV) and 296°C (1.43 uV) which gain up to ~49 and 324 mJ mg^{-1} of heat through endothermic reaction, while SA loses up to −258 mJ mg° of heat through exothermic reaction, respectively.[37] Any change in the DTG and DTA curve of the uncrosslinked as well as crosslinked film with respect to polymers indicated that addition or crosslinking of PVA/SA SHD films increased the thermal stability of PVA/SA SHD films as well as confirmed the higher cross-linking of PVA/SA SHD.[39]

Similarly, blank SHD films and SHD a film loaded with AgNPs degrades (TG) in two steps and accomplished by ~86% and ~65% weight loss [Figure 7(C,D)]. The difference in the decomposition between blank SHD and SHD film loaded with AgNPs was found ~21%. The presence of nano-silver in the hydrogel network can catalyze CO_2 elimination from polymer chain and thus delayed degradation process. However, the initial thermal degradation temperature of blank SHD and SHD/

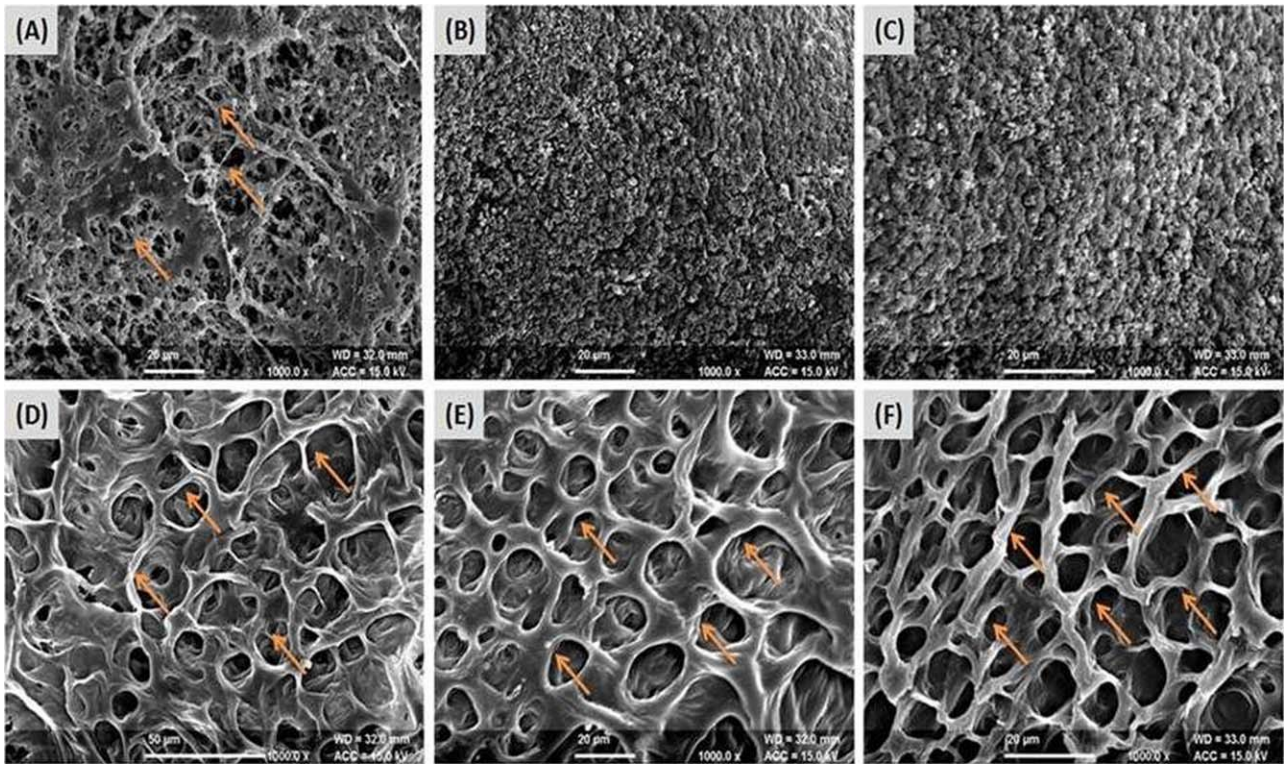

Figure 6. SEM images (A–F) depicts the surface morphology, porosity and crosslinking of PVA/SA SHD films with PVA/SA ratio varying in the range of 1:0, 0:1, 1:2, 1:1, 2:1, and 3:1 (at magnification of ×1000). [Color figure can be viewed in the online issue, which is available at wileyonlinelibrary.com.]

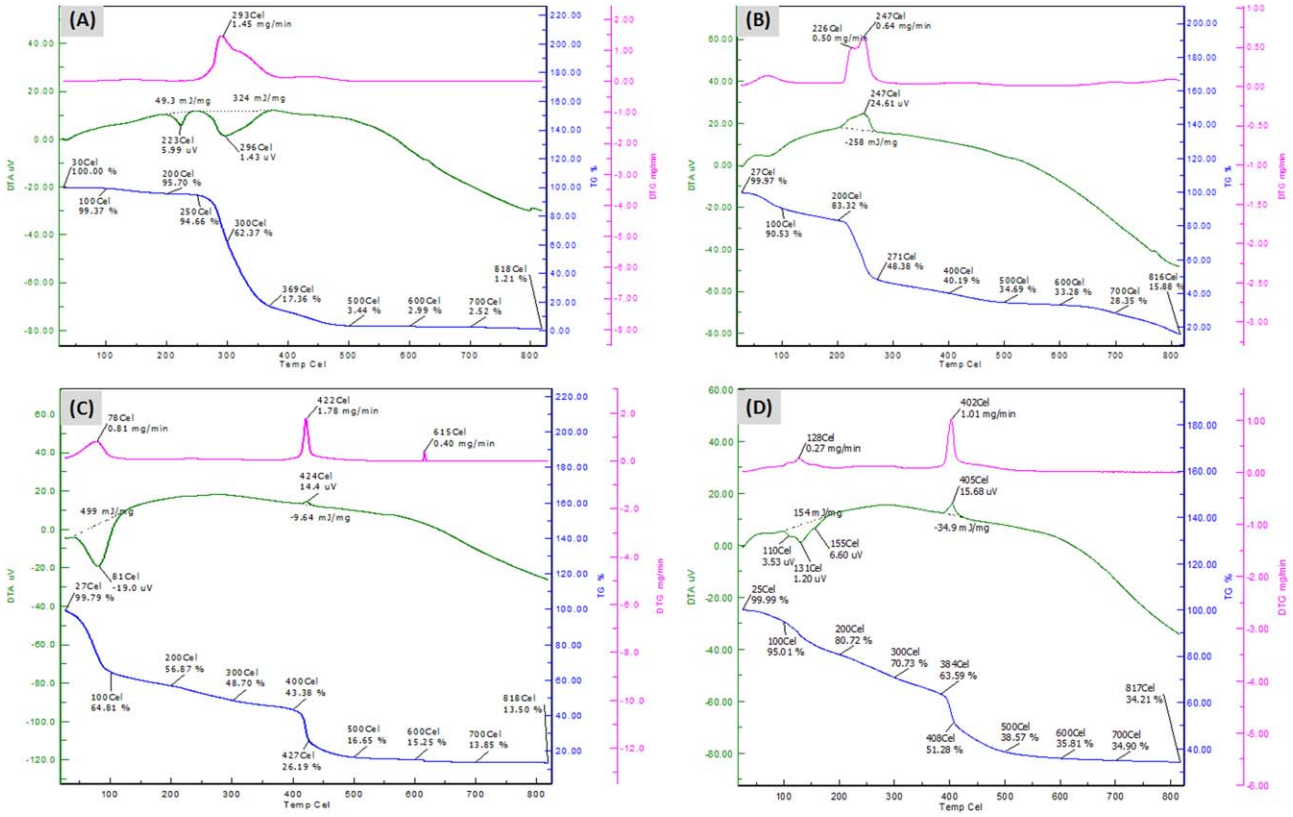

Figure 7. TGA studies showed polymeric interaction through thermal degradation behavior (A) PVA alone, (B) SA alone, (C) PVA/SA SHD, and (D) PVA/SA/Ag SHD films at a heating rate of 10°C min^{-1}. [Color figure can be viewed in the online issue, which is available at wileyonlinelibrary.com.]

AgNPs film was greater than that of homopolymers which indicates that there was a specific intermolecular interaction between PVA, SA in the blank SHD and SHD/AgNPs film.[40] The DTG and DTA curves for blank SHD films and SHD-AgNPs films showed that the thermal response features are consistent with the TGA analysis as reflected by the DTG and DTA peaks. The T_{DTG} for blank SHD films and SHD film loaded with AgNPs was found to be 422°C (1.78 mg min^{-1}) and 402°C (1.01 mg min^{-1}) respectively, which may correspond to loss of lattice water [Figure 7(C,D)]. It was observed from DTA curves that the first two stages were endothermic for blank SHD films (81°C) as well as SHD films loaded with AgNPs (131°C) which gain up to 499 and 154 mJ mg° of heat and other two stages were exothermic which loses up to −9.64 and −34.9 mJ mg° of heat, respectively [Figure 7(,D)]. Endothermicity in the first peak (for blank SHD as well as AgNPs loaded SHD) indicated that energy required vaporizing the absorbed water molecules while exothermicity means that energy released from burning of new chemical bonds.[38]

Equilibrium Swelling Ratio (ESR). Figure 8(A) depicts the effect of PVA content on the ESR with respect to different pH media. ESR decreased from 6.89 to 4.27 (1.61-fold; at pH 1.2) on decreasing the content of SA (100–66%) while ESR increased from 0.33 to 3.39 (10.27-folds; pH 1.2) on increasing PVA content (33–100%) in the PVA/SA SHD. In distilled water (DW), ESR increased from 0.71 to 4.94 (6.95-fold) with increasing PVA content from 0 to 100% while opposite results were observed at pH 7.4. ESR decreased from 4.22 to 0.93 (4.53-fold) on increasing the PVA content as above. While at pH 6.5 net ESR increased from 2.09 to 8.72 (4.17-fold) on increasing the PVA content (from 0 to 66%), whereas opposite results were obtained on increasing the content of PVA (66 to 100%) i.e., net ESR decreased from 7.99 to 2.51 (3.18-fold).

In addition, the extent of ionization of the carboxylic group of SA produces greater number of carboxylate ions along the SA polymer chain as the pH increases from 1 to 5. Because pK_a of sodium alginate is ~3.2, and most of the carboxylic group in the sodium alginate exist in unionized form (i.e., —COOH). In the shell, hydrogen bond were formed by —COOH of alginate results in the formation of stronger interaction between polymers chains and reduces the chances of surrounding liquid to diffuse into the tightly packed structure thus decreases the swelling capacity.[41] These carboxylate ions centers repels each other and produce a rapid relaxation in the hydrogel network chain which further resulting in a rise in the degree of fluid uptake. At the basic pH(DW and pH 7.4), all the —COOH groups of SA are converted to —COO^-, resulting in higher anion–anion (electrostatic) repulsion and high swelling capacity.[42] A similar behavior of low sodium alginate in acidic medium has also been reported by Deng *et al.*,[41] while high swelling at higher PVA content could be due to the hydrophilic nature and presence of hydroxyl group (—OH) in the PVA, which could have participated in the hydrogen bonding and further lead to swelling of the hydrogel in the acidic as well as basic medium.[43]

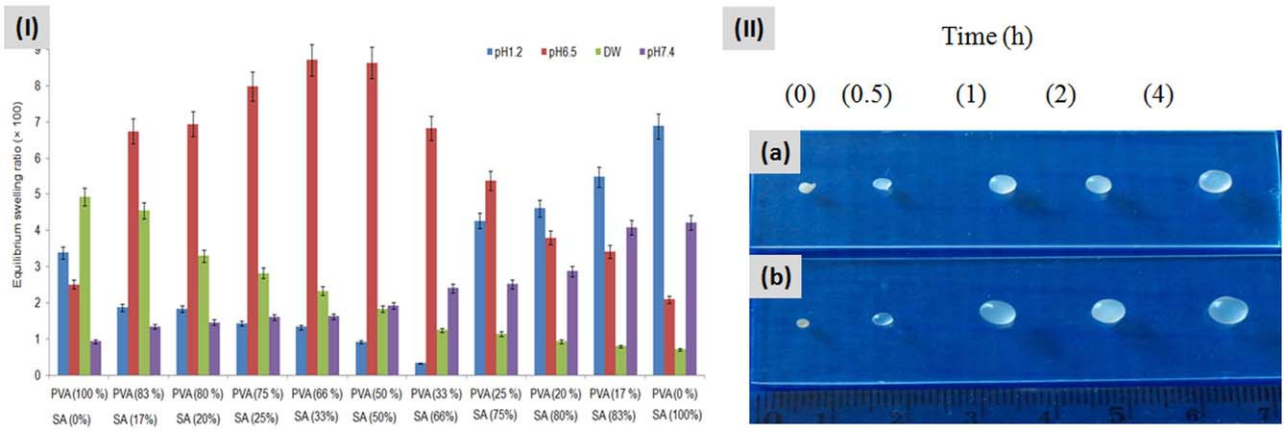

Figure 8. (I) Demonstration of the effect of PVA/SA ratio on the water uptake behavior (equilibrium swelling ratio; ESR) of PVA/SA sprayed hydrogel dressing (SHD) in distilled water, pH 1.2, 6.5, and 7.4 ($n = 5$; mean ± SD), (II) Photographs of (a) SA and (b) PVA beads showed degree of swelling after 30 min, 1, 2, and 4 h, respectively. [Color figure can be viewed in the online issue, which is available at wileyonlinelibrary.com.]

Weight Loss Profile. Figure 9(A) depicted the weight loss profile of PVA/SA SHD films under *in vitro* conditions (37°C ± 0.2°C, pH 6.5). It has been found that with increasing PVA content from 0 to 33% (and decreasing SA content from 100 to 66%) in SHD film, percentage loss in weight decreased from 89.19 to 78.98% of its total weight. Further increase in PVA content from 50 to 100%, it decreased from 73.4 to 69.81% within 72 h. Higher PVA content from 50 to 100% provide strength to the films and also reduced the degradation rate.

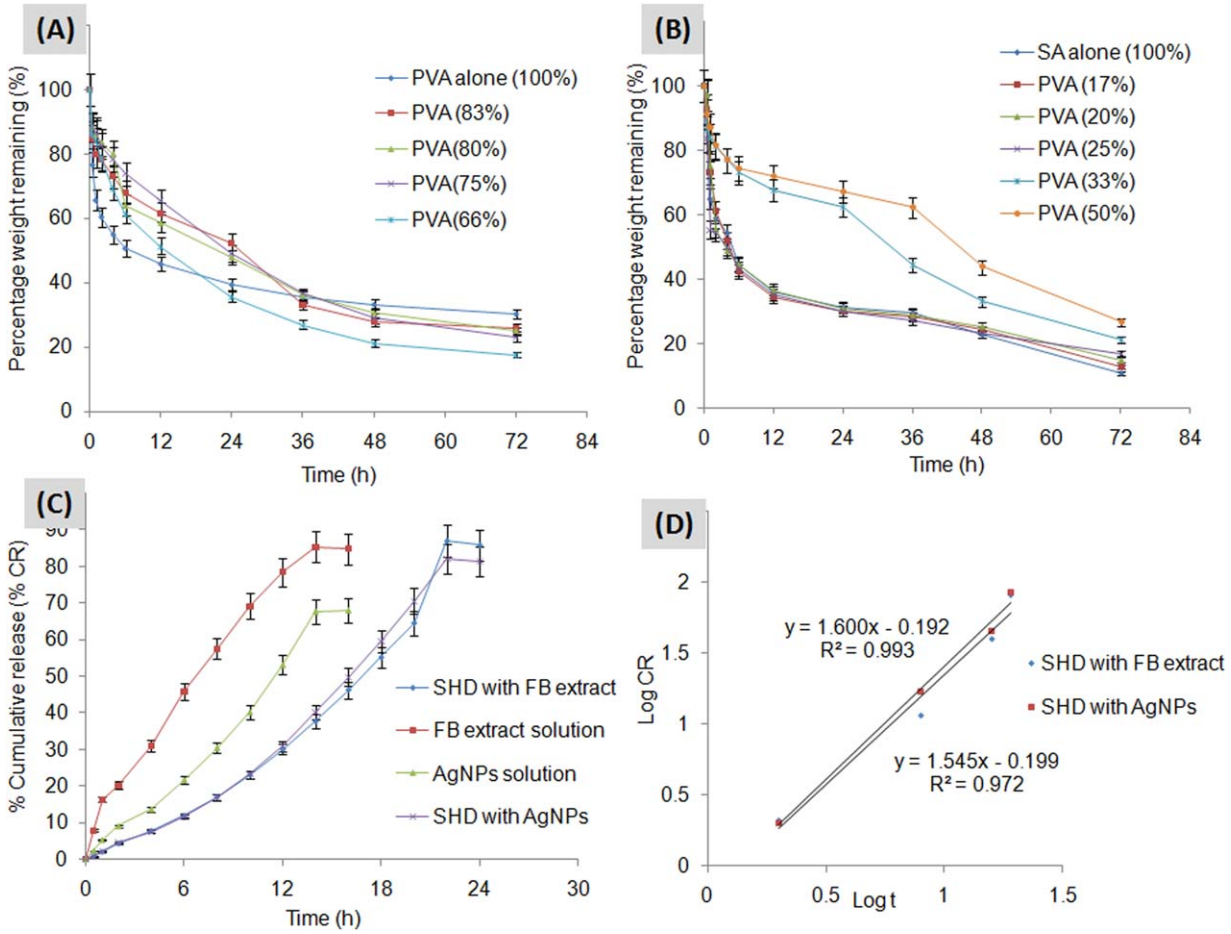

Figure 9. (A and B) Weight loss profile of PVA/SA SHD films in pH 6.5; (C and D) demonstrate release profile and release kinetics of PVA/SA SHD films (mean ± SD; $n = 5$). [Color figure can be viewed in the online issue, which is available at wileyonlinelibrary.com.]

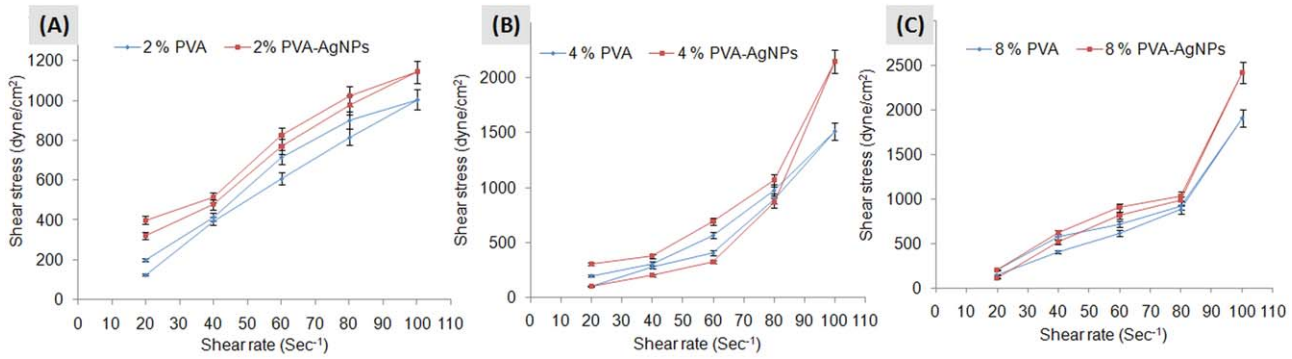

Figure 10. Rheograms of prepared PVA gel solution containing (A) 2% PVA solution and 2% PVA-AgNPs, (B) 4% PVA solution and 4% PVA-AgNPs and (C) 8% PVA solution and 8% PVA-AgNPs. [Color figure can be viewed in the online issue, which is available at wileyonlinelibrary.com.]

The higher rate of degradation with sodium alginate content can be explained on the basis of their crosslinking and water solubility (gelling ability) of SA. During cross-linking of SA with calcium chloride, Na^+ ions were substituted by Ca^{2+} ions, resulted in the formation of calcium alginate thus, exhibited higher swelling and degradation.[44] This can further explained on the basis that calcium alginate contained lower ionic cross-linking which further caused dissolution of ionic cross-linked hydrogel.[45] The lower degradation of PVA with increased ratio of PVA in the SHD i.e. (PVA/SA; 5:1) could be due to the formation of firm H-bonding among —OH groups of PVA chain.[43]

Rheological Behavior. Rheological properties of polymers are important aspect of SHD films as the knowledge of microstructural environment or mobility (fluidity) not only responsible for drug diffusion and compatibility but also useful for handling of the product.[46] The viscosity was evaluated to find the change in the properties of the synthesized gels with respect to concentration of its components (i.e., PVA alone and PVA/AgNPs). Rheogram of PVA solutions were presented in Figure 10(A–C). PVA solution exhibited pseudo-plastic flow as evidenced by Farrow's constant (>1).[47] The Farrow's constant values for 2, 4, and 8% w/v PVA and PVA-Ag solution were found to be 5.26 ± 1.23, 5.71 ± 1.45, 6.25 ± 2.1, and 6 ± 0.89, 4 ± 1.45, and 4.72 ± 0.98, respectively. Moreover, viscosity of PVA solution decreased from 915 to 468.9 cp with increase in shear stress from 200 to 1145 dyne cm^{-2} and shear rate 20–100 s^{-1}. Upon addition of 8% v/v AgNPs into PVA solution, viscosity of PVA solution increased from 515 to 1002 cp. This could be due to the electrostatic interactions between the PVA and the silver nanoparticles.[48]

It has been found that when PVA alone (without AgNPs) was used for the measurement, viscosity of PVA is less than that of PVA/Ag; this could be due to the presence of free hydroxyl group and lack of the interaction among the OH groups and Ag nanoparticles. The gels showed a pseudo-plasticity or shear thinning effect as advantageous possessions during topical applications since the gel would become more fluid. In addition, the viscosity would most likely increase when the stress ceased, avoiding the gel to flow from the site of application.[48] Rheological behavior of hydrogels depends on the concentration of the polymer and cross-linking agent which is required to be optimum for better flow properties.

Atomic Absorption Spectroscopy, Drug Loading and *In Vitro* Drug Release Studies

Three randomly selected sites from sprayed hydrogel for content uniformity (Ag) were taken in order to determine the Ag content in sprayed hydrogel and AgNPs synthesized using *FB* extract (1 mg mL^{-1}) and sodium borohydride (1 mg mL^{-1}; for comparison study). From AAS studies, 76.13 ± 0.17 mg L^{-1}, 87.05 ± 0.047 mg L^{-1} of silver was measured in samples (i.e., $AgNO_3$) synthesized by *FB* extract and sodium borohydride. While randomly selected sites of SHD discs contained average of 0.177 ± 0.008 mg g^{-1} of silver. The AAS study confirmed uniformity and considerable immobilization of silver in the PVA/SA SHD films. The percentage loading of FB extract in SHD films was found to be $89.8\% \pm 1.21\%$. Higher loading could be due to increased solubilization of *FB* extract in the polymeric system. The results of AAS suggested that uniformity of silver ion concentration in the SHD could be due to strong and uniformly interaction of silver ions with PVA and SA chain leading to higher loading and uniformity of the AgNPs in the SHD having equal PVA and SA fraction.

Figure 9(C) depicts the percentage cumulative release profile of *FB* extract as well as $AgNO_3$ from the SHD films with respect to time. It was noticed that $\sim 87\% \pm 1.78\%$ and $\sim 82\% \pm 1.67\%$ of *FB* extract and silver ions were released respectively, in a sustained manner up to 24 h from SHD films in comparison to their solution forms. The drug release kinetics was analyzed by plotting the log of cumulative release data versus log of time. According to Korsmeyer–Peppas model, the values of SHD/AgNPs and SHD/*FB* films exponent "*n*" is found to be >1 [Figure 8(D)] which indicated a super case-II transport[49] i.e., AgNPs as well as FB extract was released due to degradation of film as well as through diffusion mechanism. The initial burst release behavior may be due to fast diffusion of the AgNPs as well as FB extract from the surface of SHD films. Furthermore, higher release rate may be related to the higher swelling ratio of the SHD film under saline and the weak H-bonding interaction between silver ions and polymeric network in the PBS. Sustained release pattern (24 h) indicated that the presence of nano-silver in the SHD hydrogel network cause less swelling with respect to time. It could probably be due to the chelation

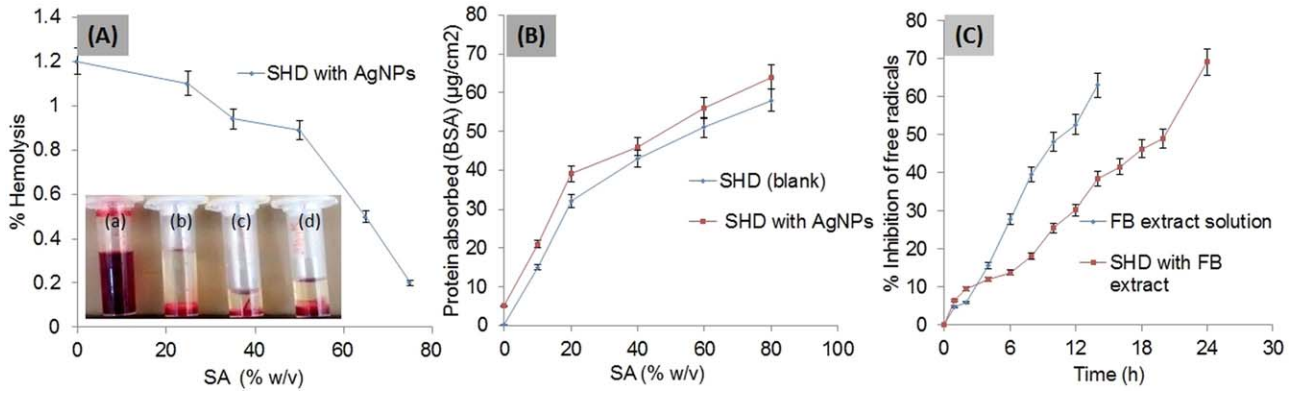

Figure 11. (A) Effect of (SA % w/v) PVA/SA SHD films on % hemolysis; Inset images (a–d) shows % hemolysis caused by Triton X (+ve control), PBS (−ve control), blank film and AgNPs-loaded film, respectively, (B) Effect of (SA % w/v) PVA/SA film on protein adsorption and (C) free radical scavenging activity of FB extract solution and extract released from PVA/SA/FB sprayed hydrogels (mean ± SD; $n = 3$). [Color figure can be viewed in the online issue, which is available at wileyonlinelibrary.com.]

of some hydroxyl group with nano-silver of the network which further neutralized the repulsions of the network causing sustained release of the silver as well as FB extract.[50]

Biological Evaluation of Hydrogel Film

Hemocompatibility and *In Vitro* Protein Adsorption Study. Figure 11(A) represents the percent hemolysis of the PVA/SA films. According to the classification of the hemolytic tendency of the polymeric material[22] it was indicated from the figure that the percentage hemolysis values decreased from 1.2 to 0.2% with increasing concentration of sodium alginate in the PVA/SA SHD films, supporting blood compatibility and non-hemolytic property of materials.

The protein adsorption on to the PVA/SA surface was calculated via *in vitro* experiments. From Figure 11(B), BSA adsorption was observed to increase from 0.2 to 58 µg cm^{-2} with increasing concentration of SA from 0 to 75% in the PVA/SA SHD films. Interestingly, the SHD films loaded with AgNPs showed a feasible adsorption of BSA in comparison to blank films. These results were also in harmony with the finding of Kamoun *et al.*, mentioned the confirmatory role of SA in enhancement of protein adsorption in SHD films.[36] When blood comes in contact with foreign materials, plasma proteins first adsorbed over their surface, which further direct the adhesion of platelets, white blood cells and red blood cells. The iso-electric point (of BSA), pK_a (of SA) and pH of blood were found to be 4.6, 4, and 7.4, respectively. In addition to that, the surface of these SHD would carry positive charge that attract negatively charged serum protein(when ionized in water at pH 7.4, as found in the body)thus exhibited higher adsorption of proteinson to the surface of SHD.[51]

***In Vitro* Hemostatic Activity.** *In vitro* coagulation time was evaluated in plastic vials to elucidate the direct effect on coagulation. In both cases, when a recalcified blood mixed with standard chitosan solution (1 mg mL^{-1}; hemostatic agent) and swollen SHD film, a coagulum occurred faster i.e., 1 min 12 s and 9 min 36 s, respectively, in comparison with control (no hemostatic activity), while, standard chitosan solution (Hemostatic agent) showed blood coagulation more than that of test as well as control. However, the amount of recalcified blood was more than that of SHD film, a delay in the coagulation of the excess blood was observed, although local aggregate formations were still continued. In both cases, coagulation time was directly depends upon the blood sample volume relative to the amount of SHD films containing *FB* extract.

The hemostatic activity of *FB* extract is due to the presence of latex (milky fluid) which is mainly responsible for hemorrhage.[52] The latex is a stable dispersion of polymer micro particles in an aqueous medium consisting of proteins, alkaloids, starches, sugar, oils, resin, and gums that coagulate along with blood on exposure to air. *FB* extract also contains a proteolytic enzyme, known as *benghalensin,*[53] which further responsible for its hemostatic or pro-coagulant activity.

***In Vitro* Free Radical Scavenging Activity.** The extract released from its solution and SHD films inhibited ∼63 ± 1.63 and ∼70% ± 1.78% of free radicals up to 14 and 24 h, respectively [Figure 11(C)]. The *in vitro* radical scavenging activity of formulations confirmed that sufficient poly-phenolic compounds were released over a period of 14 h. As oxidative stress is major hurdle towards healing of diabetic wounds, these films dressing were able to maintain anti-oxidative environment for 24 h as a crucial advantage towards healing. Phenolic compounds present in *FB* extract were mainly responsible for its antioxidant activity. Phenolic compounds fall into several categories; chief among these are the flavonoids which have potent antioxidant activity.[54] Results of this study revealed that the plant extract contains phytochemicals constituents that are capable of denoting hydrogen atom to the free radicals to scavenge the potential damage.

In Vitro* Antimicrobial Activity. *Microbe penetration and zone of inhibition study. Daily investigation of agar plates confirmed that no bacteria were passed through the sprayed hydrogel during a week. This ability of sprayed nanocomposite hydrogel dressing will protect the wound from infection and will accelerate the wound healing process. The zone of inhibition of *FB* extract, AgNPs and SHD films containing AgNPs were investigated against two bacterial strains i.e., *S. aureus* and *E. coli*

[Figure 2(E,F)]. As expected, no zone of inhibition was observed with control while with test specimens, *Staphylococcus* has shown higher zone of inhibition (16 mm) as compared to that of *E. coli* (10 mm). The size and shape of nanoparticles plays an important role for their antibacterial as well as many of the clinical applications. The observed difference in the zone of inhibition among both of the bacteria may be due to the susceptibility of the bacteria toward silver nanoparticles. Results also indicated a concentration and time dependent inhibition of bacterial zone for up to 24 h [Figure 2(G,H)].

The antimicrobial activity of silver-loaded SHD films could be attributed to the fact that silver nano-particles can interact with the sulfur-containing proteins from cell membrane and phosphorous-containing compounds in cell which further attack the respiratory chain with cell division leading to cell death.[55] It has been claimed that silver ions bind to thiol groups (—SH) in the enzyme and subsequently causes deactivation of the enzyme.[56] The use of AgNPs has exhibited phenomenal antibacterial activity due to high surface area thereby, maintained its efficacy in a sustained manner for 24 h.[57,58] Uninterrupted antimicrobial environment helps in acceleration of healing progression as sepsis is the major cause of death in chronic wounds.

CONCLUSIONS

The complexities in management of chronic wounds have been addressed via designing of an aerosolized nanocomposite hydrogel dressing of PVA and SA, which imbibes all the requisite properties and will provide an ideal healing environment along with excellent patient convenience. To evaluate the potential of these aerosols based system in wound healing application, some of very crucial *in vitro* properties such as water absorption capacity, degradation, microbe penetration assay and other biological parameters like protein adsorption and hemocompatibility were investigated. It was concluded that quantity of crosslinkers used was a key regulator (based on optimized concentration of crosslinkers) for the preparation of sprayed films with desirable properties. Because of their unique nature of application, excellent swelling, almost ~100% degradation and biocompatible nature they could be excellent candidates for wound healing process.

REFERENCES

1. Murphy, P. S.; Evans, G. R. D. *Plast. Surg. Int.* **2012**, *2012*, 1.
2. Cortivo, R.; Vindigni, V.; Lacobellis, L.; Abatangelo, G.; Pinton, P.; Zavan, B. *Nanomed.* **2010**, *5*, 1.
3. Jaiswal, M.; Gupta, A.; Dinda, K. A.; Koul, V. *J. Appl. Polym. Sci.* **2015**, *132*, 42120.
4. Yoshii, F.; Zhanshan, Y.; Isobe, K.; Shiozaki, K.; Makunchi, K. *Radiat. Phys. Chem.* **1999**, *55*, 133.
5. Wang, J.; Lin, L.; Cheng, Q.; Jiang, L. *Angew. Chem.* **2012**, *124*, 4754.
6. Kamata, H.; Akagi, Y.; Kayasuga-Kariya, Y.; Chung, U.; Sakai1, T. *Science* **2014**, *343*, 873.
7. Cheng, Q.; Jiang, L.; Tang, Z. *Acc. Chem. Res.* **2014**, *47*, 1256.
8. Sun, T. L.; Kurokawa, T.; Kuroda, S.; Ihsan, A. B.; Akasaki, T.; Sato, K.; Haque, M. A.; Nakajima, T.; Gong, J. P. *Nat. Mater.* **2013**, *12*, 932.
9. Gong, J. P.; Katsuyama, Y.; Kurokawa, T.; Osada, Y. *Adv. Mater.* **2003**, *15*, 1155.
10. Balakrishnan, B.; Mohanty, M.; Umashankar, P. R.; Jayakrishnan, A. *Biomaterials* **2005**, *26*, 6335.
11. Dong, Y.; Hassan, W.; Kennedy, R.; Greiser, U.; Pandit, A.; Garcia, Y.; Wenxin, W. *Acta Biomater.* **2014**, *10*, 2076.
12. Tran, Q. H.; Nguyen, V. Q.; Le, A. *Adv. Nat. Sci. Nanosci. Nanotechnol.* **2013**, *4*, 033001.
13. Gilchrist, T.; Martin, A. M. *Biomaterials* **1983**, *4*, 317.
14. Kasthuri, J.; Veerapandian, S.; Rajendiran, N. *Colloids Surf. B Biointerf.* **2009**, *68*, 55.
15. Sarker, S. D.; Nahar, L.; Kumarasamy, Y. *Methods* **2007**, *42*, 321.
16. Jaiswal, M.; Dinda, A. K.; Gupta, A.; Koul, V. *Biomed. Mater.* **2010**, *5*, 065014.
17. Jaiswal, M.; Naz, F.; Dinda, A. K.; Koul, V. *Biomed. Mater.* **2013**, *8*, 045004.
18. Suwantong, O.; Opanasopit, P.; Ruktanonchai, U.; Supaphol, P. *Polymer* **2007**, *48*, 7546.
19. Bonferoni, M. C.; Rossi, S.; Ferrari, F.; Caramella, C. *Pharm. Del. Technol.* **1999**, *4*, 45.
20. Chhatri, A.; Bajpai, A. K.; Shandhu, S. S.; Jain, N.; Biswas, J. *Carbohydr. Polym.* **2011**, *83*, 876.
21. Singh, D. K.; Ray, A. K. *J. Appl. Polym. Sci.* **1994**, *53*, 1115.
22. ASTM F756-00, Standard Practice for Assessment of Hemolytic Properties of Materials, ASTM International: West Conshohocken, PA, **2000**. Available at: www.astm.org.
23. Behrens, A. M.; Sikorski, M. J.; Li, T.; Wub, Z. J.; Griffith, B. P.; Kofinas, P. *Acta. Biomater.* **2014**, *10*, 701.
24. Lin, W. C.; Yu, D. J.; Yang, M. C. *Colloids Surf. B Biointerfaces.* **2006**, *47*, 43.
25. Mahdi, E. S.; Noor, A. M.; Sakeena, M. H.; Abdullah, G. Z.; Abdulkarim, M. F.; Sattar, M. A. *Int. J. Nanomed.* **2011**, *6*, 2499.
26. Kokabi, M.; Sirousazar, M.; Hassan, Z. M. *Eur. Polym. J.* **2007**, *43*, 773.
27. Perez, C.; Pauli, M.; Bezevque, P. *Acta Biol. Med. Exp.* **1990**, *15*, 113.
28. Manian, R.; Anusuya, N.; Siddhuraju, P.; Manian, S. *Food Chem.* **2008**, *107*, 1000.
29. Xu, G.; Qiao, X.; Qiu, X.; Chen, J. *Colloids Surf. A Physicochem. Eng. Aspect.* **2008**, *320*, 222.
30. Lara, H. H.; Ayala-Nunez, N. V.; Turrent, L. C. I.; Padilla, C. R. *World J. Microbiol. Biotechnol.* **2010**, *26*, 615.
31. Mandal, S.; Kumar, S. S.; Krishnamoorthy, B.; Basu, S. K. *Braz. J. Pharm. Sci.* **2010**, *46*, 785.
32. Miyazaki, T.; Takeda, Y.; Akane, S.; Itou, T.; Hoshiko, A.; En, K. *Polymer* **2010**, *51*, 5539.
33. Kim, J. O.; Park, J. K.; Kim, J. H.; Jin, S. G.; Yonga, C. S.; Li, D. X.; Choi, J. Y.; Woo, J. S.; Yoo, B. K.; Lyoo, W. S.; Kim, J. A.; Choi, H. G. *Int. J. Pharm.* **2008**, *359*, 79.

34. Silverstein, R. M.; Bassler, G. C.; Morril, T. C. Spectroscopic Identification of Organic Compounds, 5th ed.; Wiley: New York, **1991**; p 430.
35. Hemalatha, K.; Somashekarappa, H.; Somashekar, R. *Adv. Mater. Phys. Chem.* **2014**, *4*, 1.
36. Kamoun, E. A.; Kenawy, E. S.; Tamer, T. M.; El-Meligy, M. A.; Eldin, M. S. *Arab. J. Chem.* **2013**, 1.
37. Georgieva1, V.; Zvezdova, D.; Vlaev, L. *Chem. Cen. J.* **2012**, *6*, 81.
38. Zhen, H.; Xiaoxu, Y.; Xi, P.; Yulong, Z.; Meifen, F.; Qiang, Z. Thermal Degradation Study of Sodium Alginate-Zeolite 4A Composites, Proceedings of the 17th IAPRI World Conference on Packaging, China, Oct 12–15, **2010**, p 406.
39. Pierog, M.; Ostrowska-Czubenko, J.; Gierszewska-Druzynska, M. *PCACD* **2012**, *17*, 67.
40. Çaykara, T.; Demirci, S. *J. Macromol. Sci. A: Pure Appl. Chem.* **2006**, *43*, 1113.
41. Deng, K. L.; Zhong, H. B.; Tian, T.; Gou, Y. B.; Li, Q.; Dong, L. R. *Express. Polym. Lett.* **2010**, *4*, 773.
42. Reddy, P. R. S.; Rao, K. M.; Rao, K. S. V. K.; Shchipunov, Y.; Ha, C. *Macromol. Res.* **2014**, *22*, 832.
43. Bahrami, S. B.; Kordestani, S. S.; Mirzadeh, H.; Mansoori, P. *Iran. Polym. J.* **2003**, *12*, 139.
44. Jao, W.; Ho, L.; Chen, Z. *J. China Univ. Sci. Tech.* **2010**, *42*, 1.
45. Bajpai, S. K.; Sharma, S. *React. Funct. Polym.* **2004**, *59*, 129.
46. Islam, M. T.; Guez-Hornedo, N. R.; Ciotti, S.; Ackermann, C. *Pharm. Res.* **2004**, *21*, 1192.
47. Shukr, M. H.; Metwally, G. F. *Trop. J. Pharm. Res.* **2013**, *12*, 877.
48. Do-Nascimento, E. G.; Sampaio, T. B. M.; Medeiros, A. C.; De-Azevedo, E. P. *Acta Cirurgica. Brasileira* **2009**, *24*, 460.
49. Costa, P.; Lobo, J. M. S. *Eur. J. Pharm. Sci.* **2001**, *13*, 123.
50. Pourjavadi, A.; Soleyman, R.; Bardajee, G. R. *Starch Starke* **2008**, *60*, 468.
51. Huang, M.; Yang, M. *Polym. Adv. Technol.* **2010**, *21*, 561.
52. Patel, M. A.; Patel, P. K.; Patel, M. B. *Ind. J. Pharmacol.* **2010**, *42*, 214.
53. Sharma, A.; Kumari, M.; Jagannadham, M. V. *J. Agric. Food Chem.* **2009**, *57*, 11120.
54. Rice-Evans, C.; Miller, N.; Paganga, G. *Trends Plant Sci.* **1997**, *2*, 152.
55. Rai, M.; Yadav, A.; Gade, A. *Biotech. Adv.* **2009**, *27*, 76.
56. Klueh, U.; Wagner, V.; Kelly, S.; Johnson, A.; Bryers, J. D. *J. Biomed. Mater. Res. B: Appl. Biomater.* **2000**, *53*, 621.
57. Murthy, P. S. K.; Mohan, Y. M.; Varaprasada, K.; Sreedhar, B.; Raju, K. M. *J. Colloid. Int. Sci.* **2008**, *318*, 217.
58. Varaprasad, K.; Vimala, K.; Ravindra, S.; Reddy, N. G. N. *J. Mater. Sci. Mater. Med.* **2011**, *22*, 1863.